ECORFAN-Journal Taiwan 9[16]1-15: e6916115
Article

PID control for tracking A 5 DOF robotic manipulator subjected to exogenous forces

Control PID para el seguimiento de un manipulador robótico de 5 GDL bajo fuerzas exógenas

Pacheco, Jorge[a], Cortés-Vega, David[b], Sanchez-Lara, Rafael[c], Alazki, Hussain[d]

[a] Universidad Autónoma del Carmen • 0009-0000-7434-0663 • 246083
[b] Universidad Autónoma del Carmen • 0000-0002-6209-2081 • 593408
[c] Universidad Autónoma del Carmen • 0000-0001-6587-1972 • 88144
[d] Universidad Autónoma del Carmen • 0000-0002-1960-3624 • 274587

SECIHTI classification:

Area: Engineering
Field: Engineering
Discipline: Electronic Engineering
Subdiscipline: Control

https://doi.org/10.35429/EJT.2025.9.16.6.1.15
History of the article:
Received: September 11, 2025
Accepted: December 10, 2025

Abstract

In this work, a differentiator-based PID control scheme was developed and applied to a robot manipulator. It was considered that the system contains uncertainties in the payload; also, exogenous forces, such as bounded disturbances in the force torques acting on the robot joints and affecting the action of the actuators; and noise in the measurements. The control scheme was tested at the simulation level, to verify its versatility in following different three-dimensional trajectories, two curves were used in 3D space, the first a cardioid and the second a lemniscate. The differentiator used, which works in conjunction with the PID, aims to obtain a good position estimate, despite the presence of noise in the measurements. The convergence of the differentiator used is guaranteed and is referenced in this work.

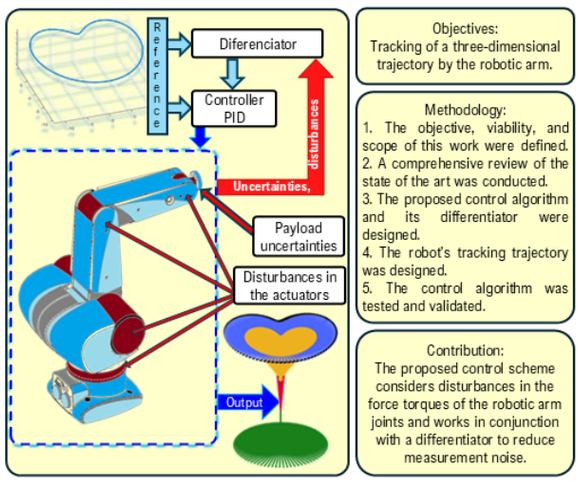

Motion control; sensorless; noises and disturbances

Resumen

En este trabajo se desarrolló un esquema de control PID basado en un diferenciador y aplicado a un Robot Manipulador. Se consideró que en el sistema existe la presencia de incertidumbres en la carga útil; asimismo la presencia de fuerzas exógenas, tales como, perturbaciones acotadas en los torques que actúan en las articulaciones del robot y afectan la acción de los actuadores; y también ruido en las mediciones. El esquema de control se probó a nivel de simulación; para verificar su versatilidad de seguimiento de trayectorias tridimensionales distintas, se utilizaron 2 curvas en el espacio 3D, la primera un cardioide y la segunda una lemniscata. El diferenciador utilizado y que trabaja en conjunto con el PID tiene como objetivo realizar una buena estimación de la posición, a pesar de la presencia de ruido en las mediciones. La convergencia del diferenciador empleado está garantizada y es referenciada en el presente trabajo.

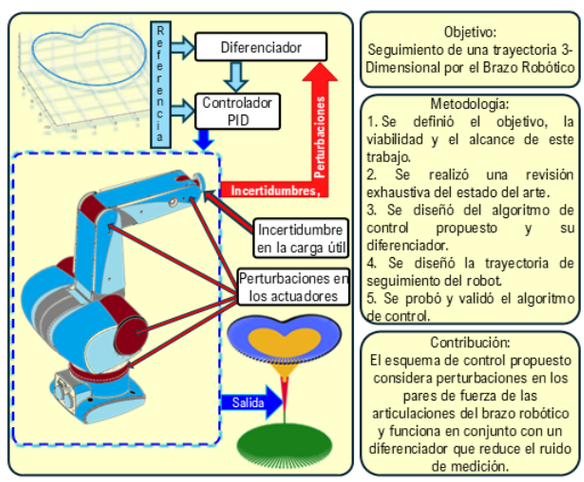

Control de movimiento; medición sin sensores; ruidos y perturbaciones

Area: Development of strategic leading-edge technologies and open innovation for social transformation

Citation: Pacheco, Jorge, Cortés-Vega, David, Sanchez-Lara, Rafael, Alazki, Hussain. [2025]. PID control for tracking A 5 DOF robotic manipulator subjected to exogenous forces. ECORFAN-Journal Taiwan. 9 [16]1-15: e6916115.

Introduction

The great importance that robotic manipulators have had in industries and in various application areas is based mainly on the core points mentioned below: efficient increase in productivity; improvement in the quality of products and processes, since precision and repeatability are a characteristic of robotic manipulators; reduction in production costs; versatility, since their programming algorithm can be changed and they can be adapted to this change to perform other tasks; safety, since they can perform highly dangerous tasks, such as transporting heavy loads or handling hazardous or contaminated materials, thus reducing the risk of occupational accidents (Álvarez et. al, 2024; Pérez, Castro, Alonso, Castillo, & Salichs, 2017).

To realize these advantages and avoid poor system performance and instability, the control algorithms designed and applied to manipulator robots must command the robotic arm to follow pre-established trajectories with a high degree of precision and speed. These characteristics must be preserved even when there are uncertainties in the mathematical model and/or perturbations in the robot's environment, such as those typically encountered in the links, the payload (Reboucas, Da Silva, Praxedes, Hemanth, & De Albuquerque, 2019) or the force torques acting on the actuator joints. It is worth mentioning that no work has been reported so far in the state-of-the-art review that considers perturbations in the force torques mentioned above.

Trajectory tracking work has been carried out with various control techniques, for example, in the area of intelligent control, work has been presented using fuzzy logic (Yilmaz, Tatlicioglu, Savran, & Alci, 2021; Urrea, & Alvarado, 2020; Bae et. al, 2017), which is useful when there is no adequate mathematical model of the system, however, some knowledge of the system dynamics is required to generate the fuzzy rules, and it is also necessary to have a large capacity of computational resources to train fuzzy or neuro-fuzzy networks (NFN), another drawback of fuzzy systems is low efficiency when the systems present uncertainties and are exposed to external disturbances; a similar thing happens in the field of neural networks (NN),

Although they have proven to be very good when there is no mathematical model of the system (Huang, Cheng, & Huang, 2023; Zhang, Zheng, Yu, Li, & Yu, 2017), they have the drawback that they require a large number of input-output data from the system to train this type of networks, which produces two other disadvantages, which are, having a large computing equipment and time to train said network; another type of intelligent control are those that use genetic algorithms (Lin, Sie, Chu, Yau, & Ding, 2021), but likewise, these require a powerful computing system, which entails an increase in the cost of the system and is sometimes not profitable; further intelligent control technique that has been used in manipulator robots is predictive control, which is based on the system model, however (Klančar, & Škrjanc 2007), this technique requires an accurate model of the system because it is sensitive to the uncertainty that arises when changes occur in the model parameters, an additional drawback is that it requires a computer to carry out the algorithm optimization process, which increases the cost of the control system.

For linear systems, or systems that are nonlinear but can be linearized around the operating point, PID controllers can be used (Božek, & Nikitin, 2021). It should be noted that its control action is only efficient in a region close to the operating point, and its efficiency decreases as it moves away from this region. PID controllers lack robustness to external disturbances that directly affect the system, and due to the uncertainties, that arise when the mathematical model does not faithfully represent the system to be controlled.

Having an exact mathematical model of the system improves the performance of most control systems. Normally, mathematical models do not fully represent the dynamics of systems and uncertainties are generated, and they may not be reliable in the presence of disturbances. A good option to overcome this problem would be to measure the variables required by the control algorithm; thus, ensuring that the control does not require a very exact model of the system.

ISSN: 2524-2121
RENIECYT-SECIHTI: 1702902

Pacheco, Jorge, Cortés-Vega, David, Sanchez-Lara, Rafael, Alazki, Hussain. [2025]. PID control for tracking A 5 DOF robotic manipulator subjected to exogenous forces. ECORFAN-Journal Taiwan. 9 [16]1-15: e6916115.
https://doi.org/10.35429/EJT.2025.9.16.6.1.15

In order not to increase the cost of the control system, instead of using sensors to measure the variables, observers (Sariyildiz & Ohnishi, 2014; Li, Yang, Chen, & Chen, 2016; Liu, Chen, Mei, & Wu, 2022; Dao, Nguyen, & Ahn, 2023) or differentiators can be used. For example, numerical differentiation (Loria, 2015; Brunot, 2019; Cao, Gan & Dai, 2019; Vo, Truong & Kang, 2021) could be useful in certain situations where the variables do not change very quickly and a high sampling rate is not required; high gain observers are another option as long as there is no high frequency noise present, since the overshoots grow greatly during transients (Stotsky, & Kolmanovsky, 2001).

There is also a type of observers that require a good mathematical model, however, precisely what is intended is not to depend too much on the model, furthermore they do not guarantee convergence in finite time (Levant, 1998); on the other hand, with the Levante differentiator the convergence in finite time can be guaranteed (Levant, 2003), when overshoots occur, they can be attenuated by means of a convenient tuning of the gains defined in its structure, furthermore they show satisfactory conditions in the case of the presence of measurement noise, and/or disturbances, and do not require large computing resources (Shtessel, Edwards, Fridman, & Levant, 2014; Na, 2019).

The Thermo CRS CataLyst 5-DOF robotic arm will track a 3-dimensional reference trajectory using a PID control scheme based on a Sliding Mode differentiator (SMD), which will allow the robot state variables required by the control algorithm to be estimated and will help eliminate the need for a highly accurate model of the system. The advantages of this differentiator structure will be leveraged to minimize undesirable effects caused by model uncertainties, as well as by the bounded perturbations that can occur at the robot manipulator joints and directly affect the torques applied to the actuators. In this way, the PID controller, working in conjunction with the aforementioned differentiator, will meet the established requirements.

The mathematical model used in this article is based on the Euler-Lagrange equations of motion.

The following sections of this work are organized as follows:

Section II mentions the methodology applied in this article; Section III describes the mathematical model used in this paper; Section IV presents the problem statement, describing SMD-based PID control algorithm, as well as mentioning the stability of the SMD; Section V presents the results obtained in this work as a result of using the aforementioned control scheme in the tracking of the 2 three-dimensional trajectories, the cardioid and the lemniscate.; Section VI describes the conclusions of this work.

Methodology

The methodology applied in this article was the following:

1. The objective, viability and scope of the research of this work were defined.
2. A exhaustive review of the state of the art was carried out.
3. The proposed control algorithm scheme was designed, as well as its differentiator.
4. The robot's tracking trajectories were proposed and designed.
5. Testing and validation of the control algorithm were carried out.

Model of the manipulator robot

A schematic drawing of the 5-DOF Thermo CRS CataLyst Robot Manipulator is presented in Figure 1, where the angles of action of each of its joints can be seen (*CRS Catalyst-5Articulated Robot*, n.d.), this robot has the following mathematical model (Okubanjo, Oyetola, Osifeko, Olaluwoye, & Alo, 2017; Lavín, Solís, Gómez, & Escobar, 2020):

$$M_i\ddot{\alpha} + M_c\dot{\alpha} + v_g = \tau(t) \quad [1]$$

In this mathematical expression:

$$\alpha \in \mathbb{R}^{5x1}, \qquad \dot{\alpha} \in \mathbb{R}^{5x1}, \qquad \ddot{\alpha} \in \mathbb{R}^{5x1}$$

are vectors representing respectively the position state, the velocity state and the acceleration of the joint angles; $\tau(t) \in \mathbb{R}^{5x1}$ is the vector of torques applied at the input of the system $M_i \in \mathbb{R}^{5x5}$; is the inertia matrix, which is symmetrical and positive definite, and depends on the manufacturer parameters *"*m, I, l, lc*"* and α, which can be expressed as follows:

$$M_i = F_{M_i}([m, I, l, lc], \alpha)$$

ISSN: 2524-2121
RENIECYT-SECIHTI: 1702902

Pacheco, Jorge, Cortés-Vega, David, Sanchez-Lara, Rafael, Alazki, Hussain. [2025]. PID control for tracking A 5 DOF robotic manipulator subjected to exogenous forces. ECORFAN-Journal Taiwan. 9 [16]1-15: e6916115.
https://doi.org/10.35429/EJT.2025.9.16.6.1.15

$M_c \in \mathbb{R}^{5x5}$ is the centripetal and Coriolis force matrix, which depends on the manufacturer parameters "m, l, lc" as well as on α and $\dot{\alpha}$, which can be written as follows:

$$M_c = F_{M_c}([m, l, lc], \alpha, \dot{\alpha})$$

$v_g \in \mathbb{R}^{5x1}$ is the vector of gravitational torques, which depends on the manufacturer parameters "g, m, l, lc" and α, which can be written as follows:

$$v_g = F_{v_g}([g, m, l, lc], \alpha)$$

g is the gravitational constant; the values of the manufacturer's parameters just mentioned are given in Table 1 and represent, "I" the inertia of the links, l" the length of the links, lc the length from the axis to the center of mass and m" the mass of the links.

It is considered that there is the presence of bounded uncertainty in the mass of the end-effector link, then the matrices M_i, M_c and the vector v_g of Eq. 1, will be affected, since they depend on the mass of the links. If it is considered that:

$$\Delta^u_{M_i}, \quad \Delta^u_{M_c}, \quad \Delta v^u_{v_g}$$

represent the increases in:

$$M_i, \quad M_c, \quad v_g$$

due to the uncertainties in the masses of the links, it can be written:

$$M^u_i = M_i + \Delta^u_{M_i},$$

$$M^u_c = M_c + \Delta^u_{M_c},$$

$$v^u_g = v_g + \Delta v^u_{v_g},$$

representing in this same order, the inertia matrix, the Coriolis matrix and centripetal forces and the gravitational force vector but already modified by the effects of the uncertainties in the masses of the links. The presence of bounded perturbations in the force torques applied to the joints of the manipulator robot will also be considered. If τ_d is considered to represent the presence of bounded disturbances in the force pairs applied to the joints, the mathematical model expressed in Eq. 1 is modified by the following expression:

$$M^u_i \ddot{\alpha} + M^u_c \dot{\alpha} + v^u_g + \tau_d = \tau(t) \qquad [2]$$

The parameters and working angles of the joints provided by the manufacturer of the Thermo CRS CataLyst 5 DOF robotic manipulator are presented in Table 1 and Table 2 respectively.

Box 1

Table 1

Parameters provided by the manufacturer of the Robot Manipulator

Link Mass (kg)	Link Length (m)	Link Inertia (kg-m^2)	Axis length to center of mass (m)
m1=5.47	l1=0.254	I1=88.22$x10^{-3}$	lc1=0.127
m2=2.09	l2=0.254	I2=33.70$x10^{-3}$	lc2=0.127
m3=1.36	l3=0.254	I3=21.93$x10^{-3}$	lc3=0.127
m4=0.006	l4=0.0508	I4=21.93$x10^{-3}$	lc4=0.0254
m5=0.6	l5=0.01	I5=39$x10^{-8}$	lc5=0.005

Source: CRS Catalyst-5Articulated Robot, n.d. https://www.equipx.net

Box 2

Table 2

Working angles of the joints provided by the manufacturer of the Robot Manipulator

values associated with the joint:				
J1	**J2**	**J3**	**J4**	**J5**
+180°/-180°	+110°/0°	+90°/-35°	+110°/-110°	+180°/-180°

Source: CRS Catalyst-5Articulated Robot, n.d. https://www.equipx.net

Box 3

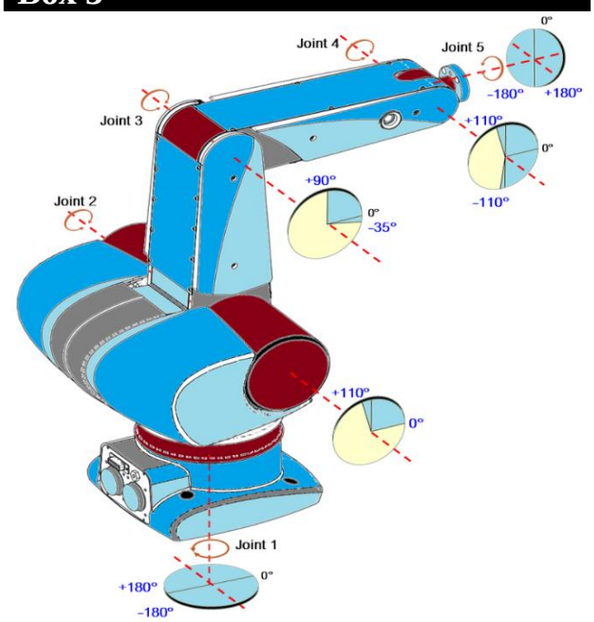

Figure 1

Manipulator Robot: Thermo CRS CataLyst 5 DOF

Source: CRS Catalyst-5Articulated Robot, n.d. https://www.equipx.net

ISSN: 2524-2121
RENIECYT-SECIHTI: 1702902

Pacheco, Jorge, Cortés-Vega, David, Sanchez-Lara, Rafael, Alazki, Hussain. [2025]. PID control for tracking A 5 DOF robotic manipulator subjected to exogenous forces. ECORFAN-Journal Taiwan. 9 [16]1-15: e6916115.
https://doi.org/10.35429/EJT.2025.9.16.6.1.15

4. Problem statement

To achieve satisfactory results with a robotic manipulator designed to perform trajectory tracking tasks in 3D space, the control algorithm used in the robot must be able to command the robotic arm's actuators to execute rapid and precise movements, even in the face of possible uncertainties in the mathematical model, such as unexpected variations in the payload of the end effector, which would directly affect the mass of the last link; as well as the presence of exogenous forces, i.e. bounded disturbances that affect the action of the actuators; noise in the force torques acting on the joints; and noise in the measurements of each of the joint angles. It is worth mentioning that the works presented with manipulator robots consider certain perturbations, but not those occurring to the force torques acting on the joints.

To address this problem, a PID control scheme will be designed in the Manipulator Robot: Thermo CRS CataLyst 5 DOF, acting in collaboration with a SMD, which will allow the system states to be estimated and at the same time its good qualities will be taken advantage of, that is, the values of the state variables will be obtained from the SMD and a high-precision mathematical model will not be necessary, its effective characteristics will also be taken advantage of when noise is present in the measurements. Figure 2 illustrates a block diagram of the proposed control scheme, and the considerations made.

Box 4

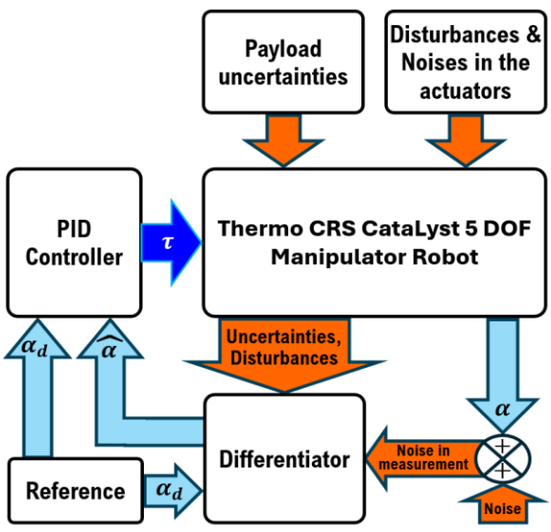

Figure 2
Block diagram of SMD-based PID control scheme.
Source: Own design and elaboration

From the following mathematical structures of the SMD Eq. 3 and Eq. 4, the position and velocity of the joint angles will be estimated:

$$\dot{\widehat{\alpha_0}} = -\lambda_1\sqrt{L}\sqrt{|\widehat{\alpha_0} - \alpha|}sign(\widehat{\alpha_0} - \alpha) + \widehat{\alpha_1} \quad [3]$$

$$\dot{\widehat{\alpha_1}} = -\lambda_0\, L\, sign\left(\widehat{\alpha_1} - \dot{\widehat{\alpha_0}}\right) \quad [4]$$

In these expressions, $\widehat{\alpha_0}$ and $\widehat{\alpha_1} \in \mathbb{R}^{5x1}$ represent the estimates of the velocity and acceleration, respectively, of the joint angles. Therefore, by integrating these equations, the position and velocity of the joint angles are obtained; $\lambda_1 > 0$ and $\lambda_0 > 0$ are parameters used to adjust the estimation of the variables; and $L > 0$ is a Lipschitz constant.

The position errors of the joint angles are obtained from Eq. 5.

$$e = \alpha_d - \widehat{\alpha_0} = x_1^d - \hat{x}_1^0 \quad [5]$$

In this expression, α_d and x_1^d represent the desired position, of the joint angles; $\widehat{\alpha_0}$ and $\hat{x}_1^0$ represent the position estimation. The position estimation errors derived from the SMD are obtained from Eq. 6.

$$e_{x_1} = x_1 - \hat{x}_1^0 \quad [6]$$

The convergence of this differentiator is demonstrated in (Levant, 1998). It can be observed how the phase trajectories of the differentiator converge. Likewise, in (Levant, 2003; Levant, 2005), the convergence of the differentiator structure is demonstrated through homogeneity properties.

The control law used, that is, the proposed PID scheme that works in conjunction with the SMD, is described below in Eq. 7:

$$\tau(t) = K_p e(t) + K_i \int e(t)dt + K_d \frac{de(t)}{dt} \quad [7]$$

In this expression K_p , K_i, & K_d, $\in \mathbb{R}^{5x1}$ represent the proportional, integral and derivative gains of the PID controller respectively, and $e \in \mathbb{R}^{5x1}$, is the tracking error, which is calculated from the estimated output position provided by the SMD, as indicated in Eq. 5.

ISSN: 2524-2121
RENIECYT-SECIHTI: 1702902

Pacheco, Jorge, Cortés-Vega, David, Sanchez-Lara, Rafael, Alazki, Hussain. [2025]. PID control for tracking A 5 DOF robotic manipulator subjected to exogenous forces. ECORFAN-Journal Taiwan. 9 [16]1-15: e6916115.
https://doi.org/10.35429/EJT.2025.9.16.6.1.15

5. Results

In this section, the results obtained from the use of a PID control scheme based on a SMD in the robotic manipulator are presented. The results shown correspond to simulations performed with MATLAB software and its Simulink Toolbox. To verify its versatility in following different three-dimensional trajectories, two curves were used in 3D space, the first a cardioid and the second a lemniscate. The tracking of the proposed trajectories will be performed with the first 4 joints of the robot, the fifth joint or end effector is used for the working angle with the payload, therefore, it is not part of the trajectory and will be proposed arbitrarily within its operating range.

The tuned gains for the PID that are expressed in Eq. 7, as well as the parameters expressed in Eq. 3, and Eq. 4 that correspond to the SMD, which were obtained to track the trajectories are shown in Table 3 and Table 4 respectively.

Box 5

Table 3
Tuned PID gains

	values associated with the joint:				
	1	**2**	**3**	**4**	**5**
K_p	675	600	600	600	$8x10^{-4}$
K_i	7.5	7.5	7.5	7.5	$5x10^{-6}$
K_d	57.75	66	40	20	$4x10^{-5}$

Source: Own design and elaboration

The graphs obtained from the simulation results of testing the SMD-based PID control algorithm on the 5-DOF Thermo CRS CataLyst robot manipulator model while tracking the 3D reference trajectories are presented below.

In the test performed with the aforementioned control scheme, the following conditions are considered:

a) Unknown, sudden, and bounded variations in the end-effector load.

b) The presence of noise in the measurements of the five joints.

c) Presence of external and bounded disturbances in the actuators that act on the first four joints of the robot.

d) Presence of noise in the force torques acting on the joints.

Box 6

Table 4
Tuned parameters corresponding to the SMD.

	values associated with the joint:				
	1	**2**	**3**	**4**	**5**
λ_1	3.06	1.836	1.836	1.224	1.652
λ_0	0.94	1.81	1.81	18.1	0.073
L	1250	1500	1375	1000	1000

Source: Own design and elaboration

Figure 3 shows the bounded uncertainty applied to the mass of the end-effector, or payload. The uncertainty was limited to 1 kg, as this is the maximum working load indicated in the manufacturer's specifications.

Box 7

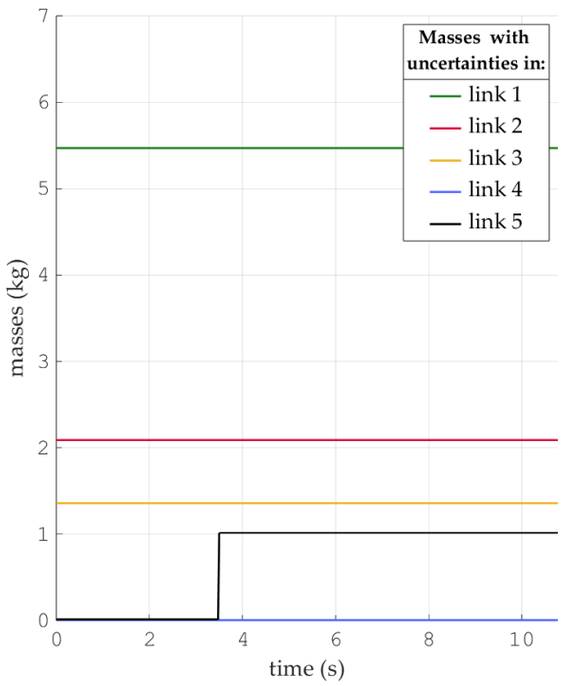

Figure 3
Graph of the bounded uncertainty applied to the mass of the 5th link or end effector
Source: Own design and elaboration.

Figure 4 shows the noises that were present in the angle measurements of the five joints.

Figure 5 shows the disturbances present in the actuators that operate on the joints of the robotic manipulator. These perturbations, as mentioned above, are external and bounded.

ISSN: 2524-2121
RENIECYT-SECIHTI: 1702902

Pacheco, Jorge, Cortés-Vega, David, Sanchez-Lara, Rafael, Alazki, Hussain. [2025]. PID control for tracking A 5 DOF robotic manipulator subjected to exogenous forces. ECORFAN-Journal Taiwan. 9 [16]1-15: e6916115.
https://doi.org/10.35429/EJT.2025.9.16.6.1.15

Box 8

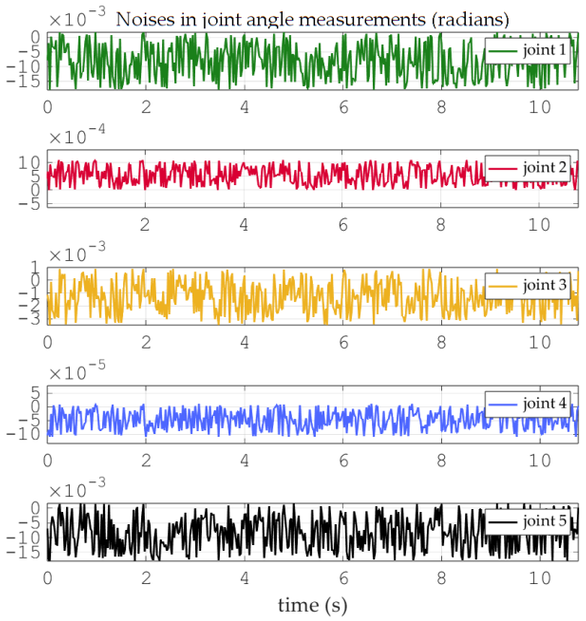

Figure 4

Graphs of the noises present at the time of joint angle measurements.

Source: Own design and elaboration.

Box 9

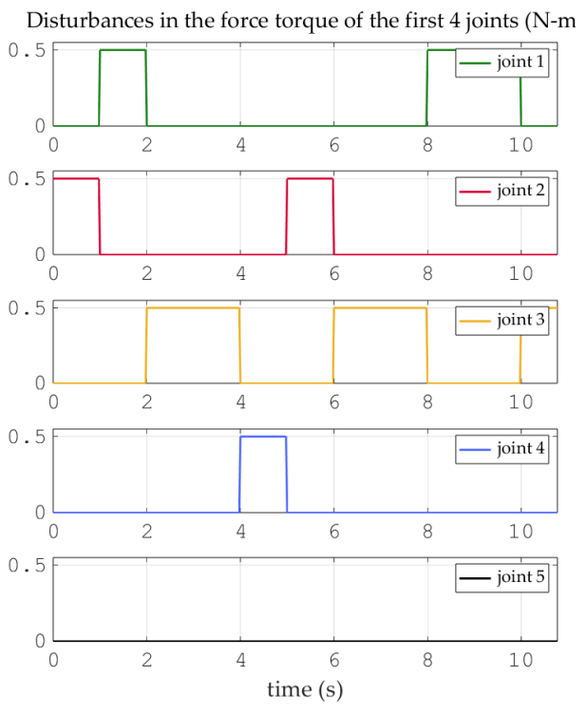

Figure 5

Graphs of the external and bounded disturbances affecting the torques of the first 4 joints of the manipulator robot

Source: Own design and elaboration

Figure 6 shows the graphs of the presence of noise in the five joints of the manipulator robot.

Box 10

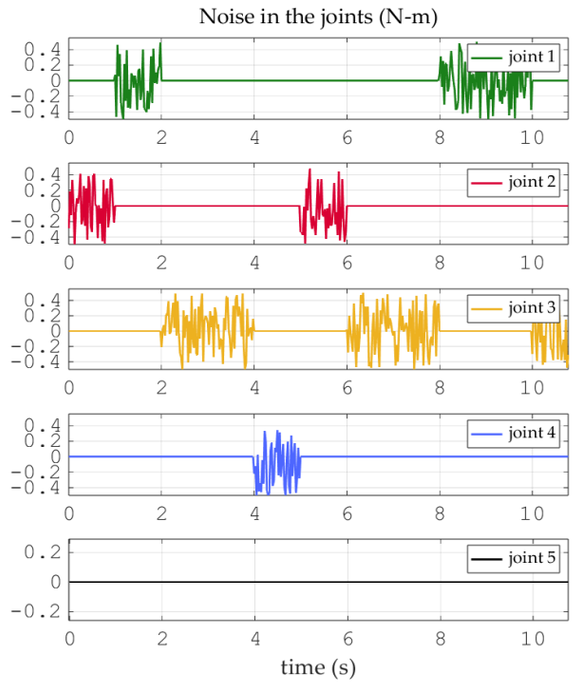

Figure 6

Graph of the presence of noise in the five joints of the manipulator robot

Source: Own design and elaboration

A) Simulations with the 3D cardioid

Figures 7 show an ideal reference trajectory for the cardioid, but they do not consider the intrinsic limitations of the manipulator robot, so it should not be used as shown. Therefore, an adjustment was made so that the manipulator robot can track said trajectory optimally without having to suffer mechanical overstress and at the same time excessive overshoots do not occur (Feng, Dai, Zhou, Xu & Wang, 2024; Haselirad & Neubert, 2014). Figure 8 shows the reference trajectory to be used, and Figure 9 shows the reference angles for each joint that form the 3D reference trajectory in Figure 8.

Figure 10 shows the graph describing the robotic manipulator as it tracks the trajectory presented in Figure 8.

Figure 11 shows the tracking of the 5 joint angles that describe the trajectory of the 3D cardioid represented in Figure 8. The angles of the desired trajectory are shown as dashed segments, and the corresponding tracking with solid segments. This graph shows that, after approximately 0.6s, accurate tracking of the reference angles for all 5 joints is achieved. A slight overshoot in the angle of the fifth joint is also observed when there is a sudden change in the reference angle of the first.

ISSN: 2524-2121
RENIECYT-SECIHTI: 1702902

Pacheco, Jorge, Cortés-Vega, David, Sanchez-Lara, Rafael, Alazki, Hussain. [2025]. PID control for tracking A 5 DOF robotic manipulator subjected to exogenous forces. ECORFAN-Journal Taiwan. 9 [16]1-15: e6916115.
https://doi.org/10.35429/EJT.2025.9.16.6.1.15

Box 11

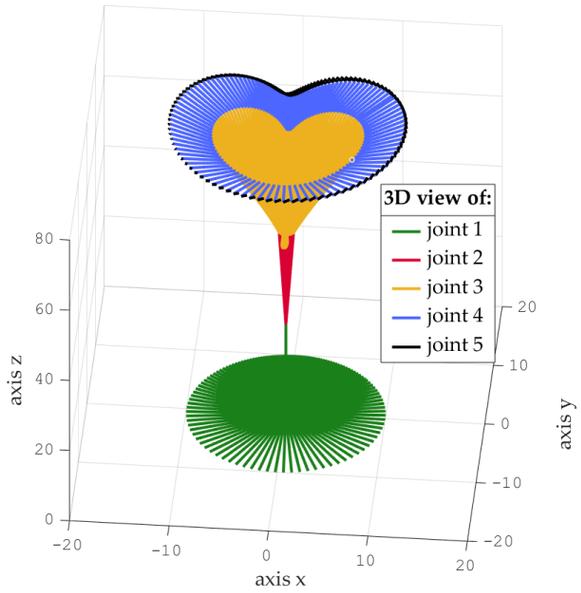

Figure 7

Ideal 3D reference trajectory of the cardioid.

Source: Own design and elaboration.

Box 12

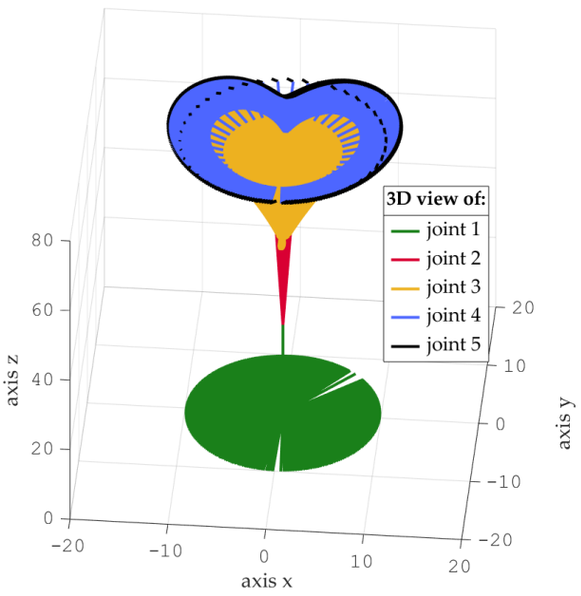

Figure 8

3D reference trajectory used for the cardioid.

Source: Own design and elaboration

Figure 12 shows the tracking error graphs for each of the angles corresponding to the 5 joints of the robotic manipulator. The errors are expressed in radians. In these graphs, it is observed that the tracking errors for each of the 5 angles always converge to zero, even though the system is permanently subject to noise in the force torques, as well as to noise in the measurements and the presence of disturbances in said torques.

It is also observed that the convergence remains towards zero when a sudden change in the trajectory of the first joint occurs, this arises in at 7.5 and 8.5 seconds. The percentage tracking error at steady state for each angle of the five joints is shown in Table 5.

Box 13

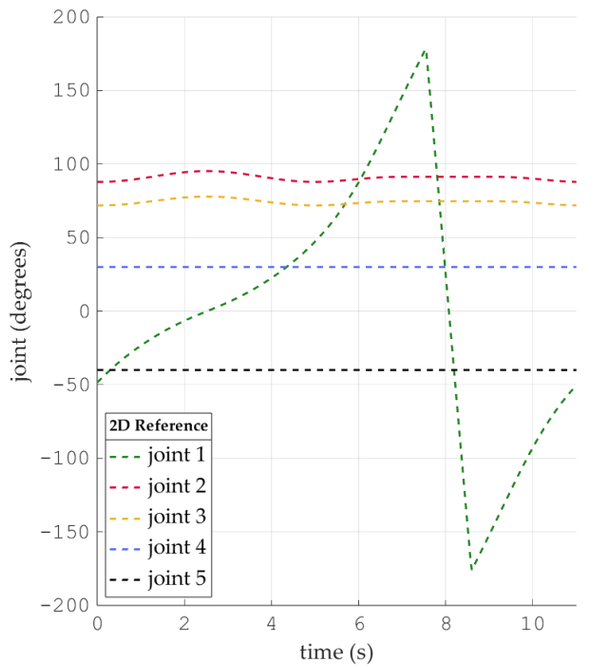

Figure 9

Graphs of the reference angles of each joint for the cardioid.

Source: Own design and elaboration

Box 14

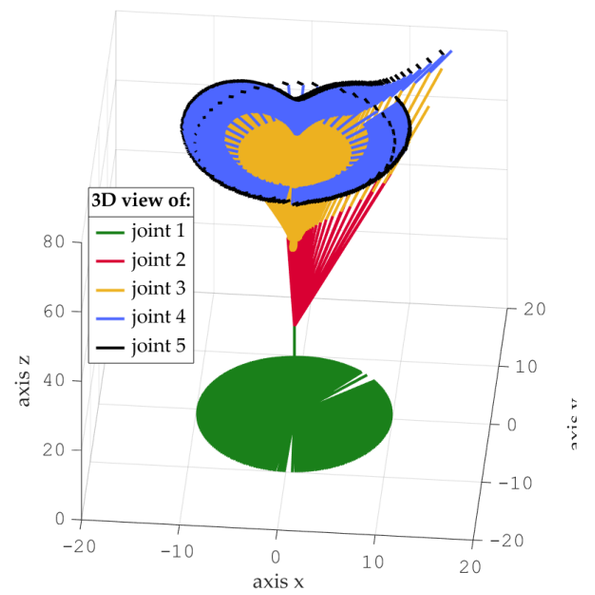

Figure 10

3D cardioid reference trajectory tracking.

Source: Own design and elaboration

ISSN: 2524-2121
RENIECYT-SECIHTI: 1702902

Pacheco, Jorge, Cortés-Vega, David, Sanchez-Lara, Rafael, Alazki, Hussain. [2025]. PID control for tracking A 5 DOF robotic manipulator subjected to exogenous forces. ECORFAN-Journal Taiwan. 9 [16]1-15: e6916115.
https://doi.org/10.35429/EJT.2025.9.16.6.1.15

Box 15

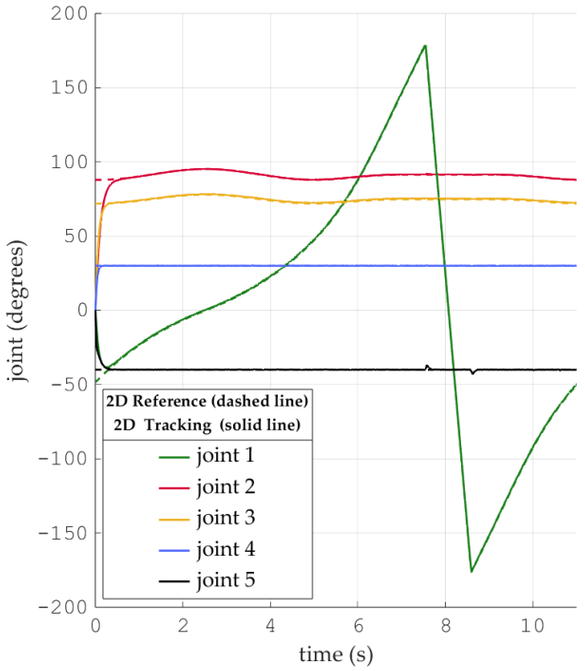

Figure 11

Graphs of the angles of the desired trajectory of the cardioid and its tracking for each joint.

Source: Own design and elaboration

Box 16

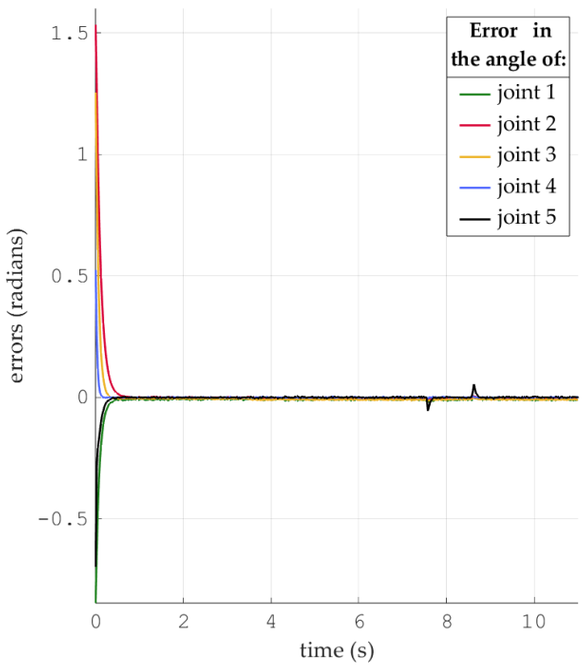

Figure 12

Graphs of the cardioid tracking errors for each of the 5 joint angles.

Source: Own design and elaboration

The percentage of steady-state tracking error for each angle of the five joints is shown in Table 5. Figure 13 shows the graphs of the estimated errors in the angles of the 5 joints using the SMD.

Box 17

Table 5

Percentage of tracking error in steady state for each angle of the 5 joints that make up the cardioid

values associated with the joint (%):				
J1	**J2**	**J3**	**J4**	**J5**
0.6614	0.1435	0.621	0.1974	0.3245

Source: Own design and elaboration.

Box 18

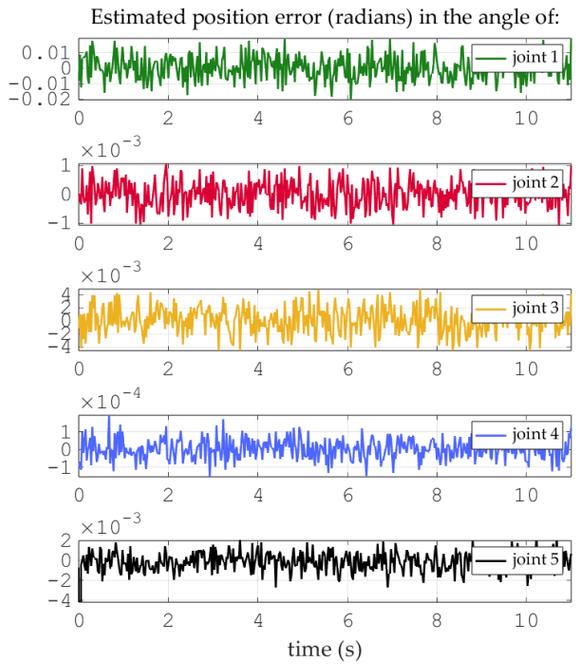

Figure 13

Graphs of the position measurement errors resulting from the estimate made by the SMD when tracking the cardioid.

Source: Own design and elaboration

The percentage error in the estimation of each of the 5 angles is shown in Table 6.

Box 19

Table 6

Percentage error of position measurement made by the estimator.

values associated with the joint (%):				
J1	**J2**	**J3**	**J4**	**J5**
305.5×10^{-3}	4.986×10^{-3}	63.96×10^{-3}	6.04×10^{-3}	97.41×10^{-3}

Source: Own design and elaboration.

Figure 14 shows the control signal, that is, the force torques applied in tracking the trajectory of the robotic manipulator.

ISSN: 2524-2121
RENIECYT-SECIHTI: 1702902

Pacheco, Jorge, Cortés-Vega, David, Sanchez-Lara, Rafael, Alazki, Hussain. [2025]. PID control for tracking A 5 DOF robotic manipulator subjected to exogenous forces. ECORFAN-Journal Taiwan. 9 [16]1-15: e6916115.
https://doi.org/10.35429/EJT.2025.9.16.6.1.15

Box 20

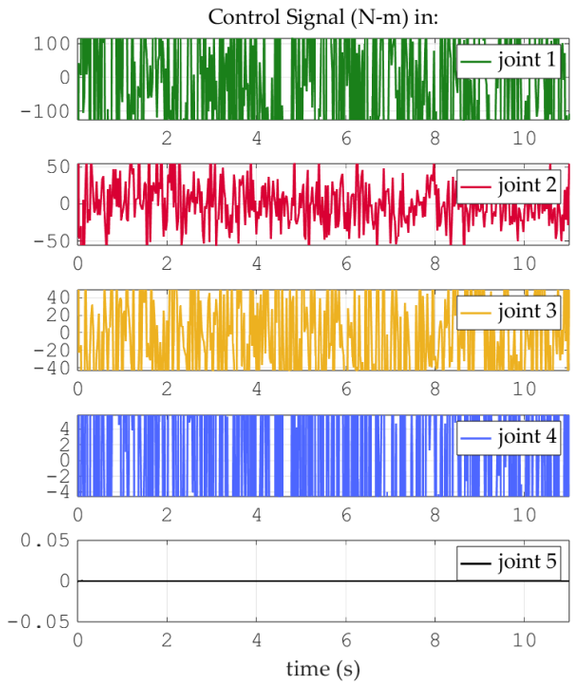

Figure 14

Graphs of the control signal applied to each joint in cardioid tracking.

Source: Own design and elaboration.

B) Simulations with the 3D lemniscate.

Figure 15 shows an ideal reference trajectory for the lemniscate, but it does not consider the intrinsic limitations of the manipulator robot. Therefore, an adjustment was made so that the manipulator robot could optimally follow this trajectory without suffering mechanical overexertion and, at the same time, avoid excessive overshoots.

Figure 16 shows the reference trajectory to be used, and Figure 17 shows the reference angles for each joint that form the 3D reference trajectory in Figure 16.

Figure 18 shows the graph describing the robotic manipulator as it tracks the trajectory presented in Figure 16.

Figure 19 shows the tracking of the five joint angles that describe the 3D lemniscate trajectory represented in Figure 16. The desired trajectory angles are shown as dashed segments, and the corresponding tracking angles are shown as solid segments. This graph shows that, after approximately 0.65s, accurate tracking of the reference angles for all five joints is achieved. A slight overshoot in the angle of the fifth joint is also observed when there is a sudden change in the reference angle of the first.

Box 21

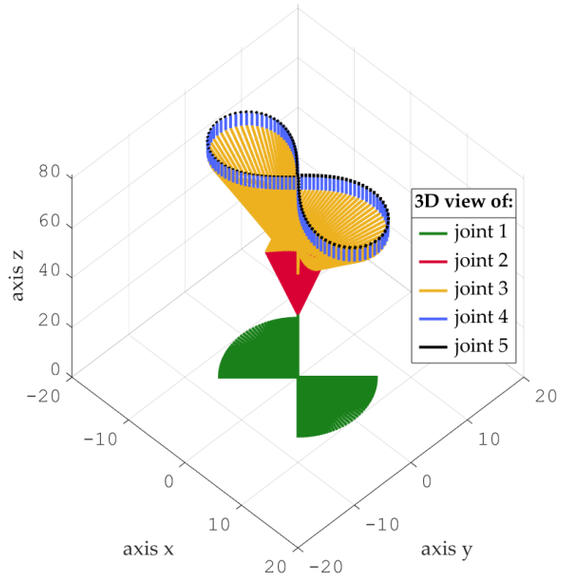

Figure 15

Ideal 3D reference trajectory of the lemniscate.

Source: Own design and elaboration

Box 22

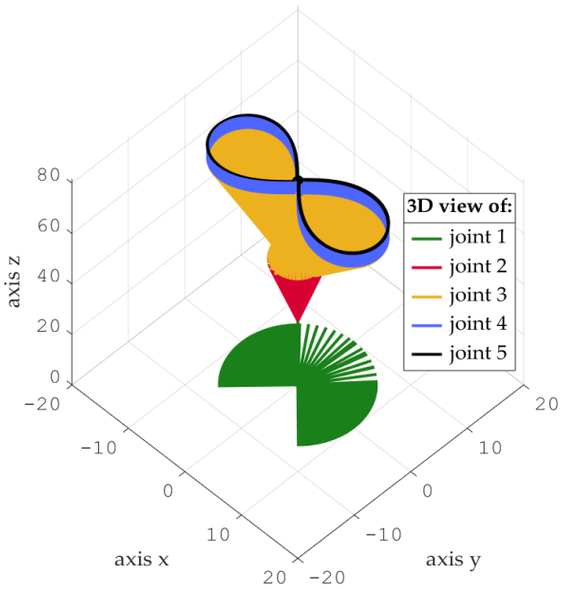

Figure 16

3D reference trajectory used for the lemniscate.

Source: Own design and elaboration.

Figure 20 shows the tracking error graphs for each of the angles corresponding to the 5 joints of the robotic manipulator. In these graphs, it is observed that the tracking errors for each of the 5 angles always converge to zero, even though the system is permanently subject to noise in the force torques, as well as to noise in the measurements and the presence of disturbances in said torques. It is also observed that convergence remains towards zero when a sudden change occurs in the trajectory of the first joint, this arises at 5 seconds and 6 seconds.

ISSN: 2524-2121
RENIECYT-SECIHTI: 1702902

Pacheco, Jorge, Cortés-Vega, David, Sanchez-Lara, Rafael, Alazki, Hussain. [2025]. PID control for tracking A 5 DOF robotic manipulator subjected to exogenous forces. ECORFAN-Journal Taiwan. 9 [16]1-15: e6916115.
https://doi.org/10.35429/EJT.2025.9.16.6.1.15

Box 23

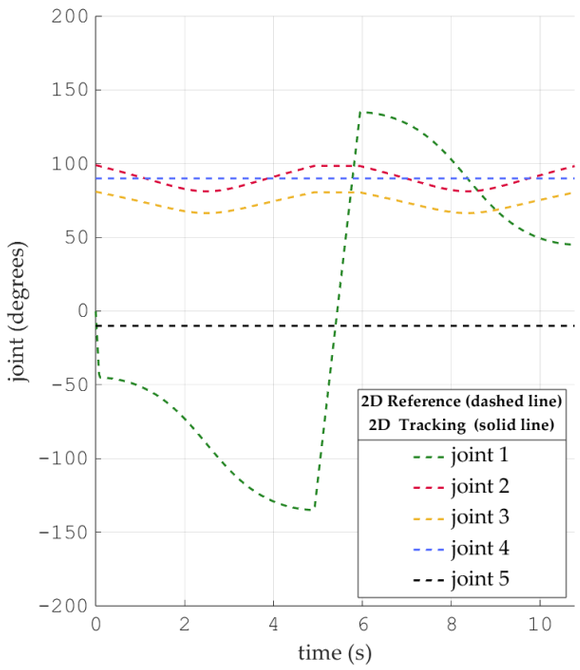

Figure 17

Graphs of the reference angles of each joint for the lemniscate.

Source: Own design and elaboration

Box 24

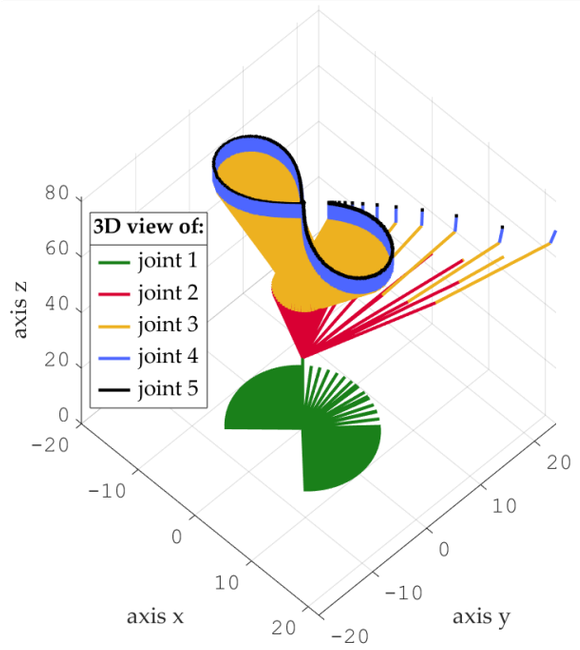

Figure 18

Tracking the reference trajectory of the 3D lemniscate.

Source: Own design and elaboration

Box 25

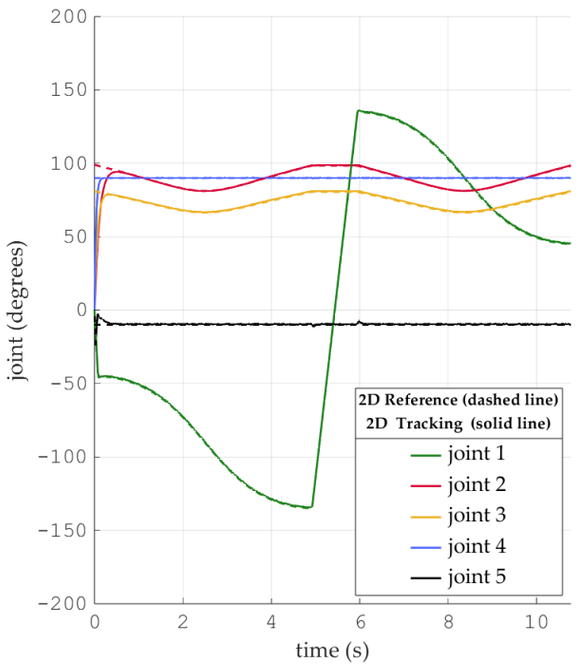

Figure 19

Graphs of the angles of the desired trajectory of the lemniscate and its tracking for each joint

Source: Own design and elaboration

Box 26

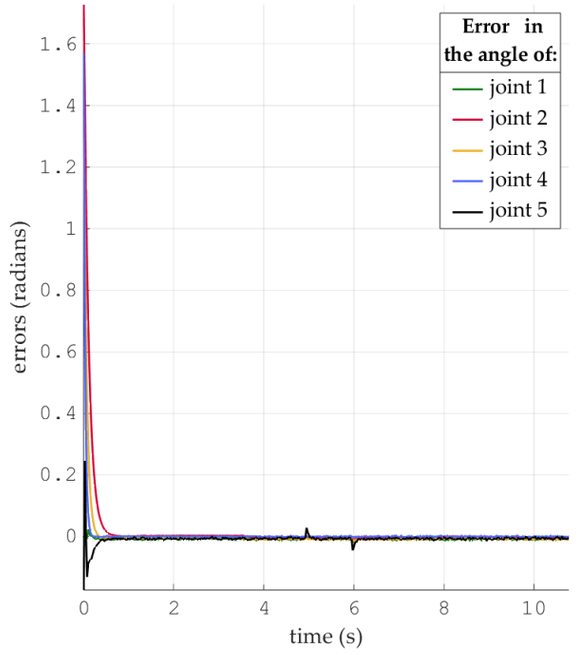

Figure 20

Graphs of the lemniscate tracking errors for each of the 5 joint angles.

Source: Own design and elaboration

The percentage of steady-state tracking error for each angle of the five joints is shown in Table 7.

ISSN: 2524-2121
RENIECYT-SECIHTI: 1702902

Pacheco, Jorge, Cortés-Vega, David, Sanchez-Lara, Rafael, Alazki, Hussain. [2025]. PID control for tracking A 5 DOF robotic manipulator subjected to exogenous forces. ECORFAN-Journal Taiwan. 9 [16]1-15: e6916115.
https://doi.org/10.35429/EJT.2025.9.16.6.1.15

Box 27

Table 7

Percentage of tracking error in steady state for each angle of the 5 joints that form the lemniscate.

values associated with the joint (%):				
J1	**J2**	**J3**	**J4**	**J5**
0.5379	0.1693	0.6350	0.0742	1.1310

Source: Own design and elaboration

Figure 21 shows the graphs of the estimated errors in the angles of the 5 joints using the SMD. The percentage error in the estimation of each of the 5 angles is shown in Table 8.

Box 28

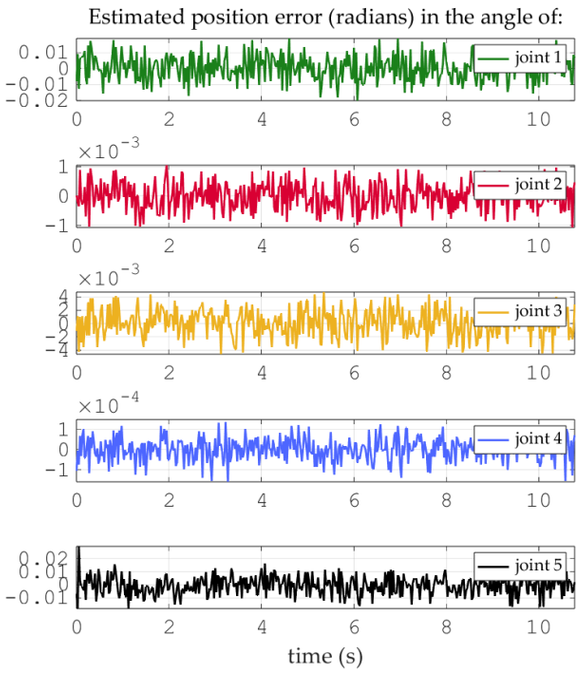

Figure 21

Graphs of the position measurement errors resulting from the estimation made by the SMD when tracking the lemniscate.

Source: Own design and elaboration

Box 29

Table 8

Percentage error of position measurement made by the SMD

values associated with the joint (%):				
J1	**J2**	**J3**	**J4**	**J5**
228×10^{-3}	5.076×10^{-3}	64.36×10^{-3}	2.173×10^{-3}	393.5×10^{-3}

Source: Own design and elaboration

Figure 22 shows the control signal, that is, the force torques applied in tracking the trajectory of the robotic manipulator.

Box 30

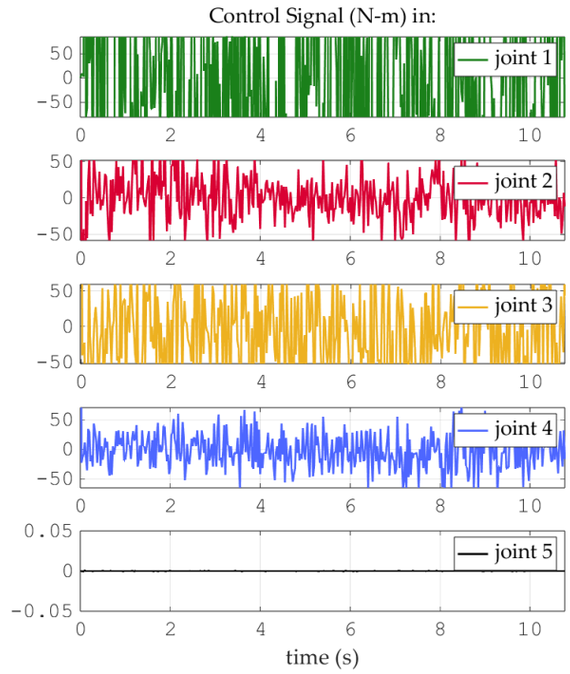

Figure 22

Graphs of the control signal applied to each joint in the tracking of the lemniscate.

Source: Own design and elaboration

6. Conclusions

A SMD-based PID control scheme was applied at the simulation level to the Thermo CRS CataLyst 5-degree-of-freedom robotic manipulator. To verify the tracking versatility of the control scheme, two three-dimensional trajectories were employed: the first a cardioid and the second a lemniscate.

Simulation tests were performed considering the following: Uncertainties in end-effector payload; the presence of noise in the measurements of the five joints; presence of exogenous forces, i.e. bounded disturbances in the actuators acting on the first 4 joints of the robot and noise in the torques acting on the joints.

It was verified that the SMD performed an excellent estimation of the states while the system tracked the proposed trajectories. The stability of SMD is guaranteed and was mentioned in this work.

ISSN: 2524-2121
RENIECYT-SECIHTI: 1702902

Pacheco, Jorge, Cortés-Vega, David, Sanchez-Lara, Rafael, Alazki, Hussain. [2025]. PID control for tracking A 5 DOF robotic manipulator subjected to exogenous forces. ECORFAN-Journal Taiwan. 9 [16]1-15: e6916115.
https://doi.org/10.35429/EJT.2025.9.16.6.1.15

Furthermore, the percentage tracking errors were found to be very small. It was also observed that the control signals obtained for tracking did not exhibit excessive overshoots. After testing and validating the control scheme, it can be determined that the development proposed in this work offers a solution to the needs previously expressed in the problem statement.

Annexes

Declarations

Conflict of interest

As authors of this research article, we declare no conflicts of interest. We have no known financial conflicts of interest or personal relationships that could have influenced the article submitted to this journal.

Author contribution

Pacheco, Jorge: He developed the proposed research; conducted an exhaustive search of the state of the art; designed the tracking trajectories, cardioid and lemniscate; tested and validated the complete control algorithm; and wrote the article.

Alazki, Hussein: He contributed the main research proposal, the method and the control technique applied in the robotic manipulator and also participated in reviewing the article's writing.

Cortés Vega, David: He tested and fine-tuned the complete control algorithm; tested and validated the structures of various differentiators for application in the control scheme; and participated in reviewing the article's editorial work.

Availability of data and materials

The control algorithm, data and graphs presented in this work were obtained from MATLAB® R2024a/Simulink version 24.1, (Natick, MA, USA) Software, are available for sharing upon request.

Funding

This research did not receive funding from any institution.

Abbreviations

3D	Three dimensions.
DOF	Degrees Of Freedom.
GDL	Degrees Of Freedom, in Spanish.
PID	Proportional Integral Derivative.
SMD	Sliding Mode Differentiator.

References

Basics

Alvarez-Sánchez, E. J., Aldana-Franco, F., Leyva-Retureta, J. G., Aldana-Franco, R., Villafuerte-Segura, R., & Domínguez-Ramírez, O. A. (2024). Tendencias Actuales en el Desarrollo de la Robótica en México. Pädi Boletín Científico de Ciencias Básicas e Ingenierías del ICBI, 12(Especial2), I-IV. DOI: 10.29057/icbi.v12iEspecial2.12560.

Bae, H. J., Jin, M., Suh, J., Lee, J. Y., Chang, P. H., & Ahn, D. S. (2017). Control of robot manipulators using time-delay estimation and fuzzy logic systems. Journal of Electrical Engineering and Technology, 12(3), 1271-1279. DOI: 10.5370/jeet.2017.12.3.1271.

Božek, P., & Nikitin, Y. The Development of an Optimally-Tuned PID Control for the Actuator of a Transport Robot. Actuators 2021, 10, 195. DOI: 10.3390/act10080195.

Brunot, M. (2019). Comparison of Numerical Differentiation Techniques for Aircraft Identification. Journal of Aerospace Engineering, 32(5), 06019002. DOI: 10.1061/(ASCE)AS.1943-5525.0001003

Cao, P., Gan, Y., & Dai, X. (2019). Finite-time disturbance observer for robotic manipulators. Sensors, 19(8), 1943. DOI: 10.3390/s19081943

CRS Catalyst-5Articulated Robot, n.d. https://acortar.link/Gx5RWx

Dao, H. V., Nguyen, M. H., & Ahn, K. K. (2023). Nonlinear functional observer design for robot manipulators. Mathematics, 11(19), 4033. DOI: 10.3390/math11194033

Feng, M., Dai, J., Zhou, W., Xu, H., & Wang, Z. (2024). Kinematics analysis and trajectory planning of 6-DOF hydraulic robotic arm in driving side pile. Machines, 12(3), 191. DOI: 10.3390/machines12030191.

ISSN: 2524-2121
RENIECYT-SECIHTI: 1702902

Pacheco, Jorge, Cortés-Vega, David, Sanchez-Lara, Rafael, Alazki, Hussain. [2025]. PID control for tracking A 5 DOF robotic manipulator subjected to exogenous forces. ECORFAN-Journal Taiwan. 9 [16]1-15: e6916115.
https://doi.org/10.35429/EJT.2025.9.16.6.1.15

Haselirad, A., & Neubert, J. (2014). A comparison of three trajectory planning methods for smooth motion in 5-DOF manipulators. *tC*, *60*(24), 6.

Huang, H. L., Cheng, M. Y., & Huang, T. Y. (2023). A rapid base parameter physical feasibility test algorithm for industrial robot manipulator identification using a recurrent neural network. IEEE Access, 11, 145692-145705. DOI: 10.1109/ACCESS.2023.3344490.

Klančar, G., & Škrjanc, I. (2007). Tracking-error model-based predictive control for mobile robots in real time. Robotics and autonomous systems, 55(6), 460-469. DOI: 10.1016/j.robot.2007.01.002.

Lavín-Delgado, J. E., Solís-Pérez, J. E., Gómez-Aguilar, J. F., & Escobar-Jiménez, R. F. (2020). Trajectory tracking control based on non-singular fractional derivatives for the PUMA 560 robot arm. Multibody System Dynamics, 50(3), 259-303. DOI: 10.1007/s11044-020-09752-y.

Levant, A. (2005). Homogeneity approach to high-order sliding mode design. Automatica, 41(5), 823-830. DOI: 10.1016/j.automatica.2004.11.029.

Levant, A. (2003). Higher-order sliding modes, differentiation and output-feedback control. International journal of Control, 76(9-10), 924-941. DOI: 10.1080/0020717031000099029.

Levant, A. (1998). Robust exact differentiation via sliding mode technique. automatica, 34(3), 379-384. DOI:10.1016/s0005-1098(97)002094.

Li, S., Yang, J., Chen, W. H., & Chen, X. (2016). *Disturbance observer-based control: methods and applications*. CRC press.

Lin, C. J., Sie, T. Y., Chu, W. L., Yau, H. T., & Ding, C. H. (2021, March). Tracking control of pneumatic artificial muscle-activated robot arm based on sliding-mode control. In Actuators (Vol. 10, No. 3, p. 66). MDPI. DOI: 10.3390/act10030066.

Liu, Y., Chen, X., Mei, Y., & Wu, Y. (2022). Observer-based boundary control for an asymmetric output-constrained flexible robotic manipulator. *Science China. Information Sciences*, *65*(3), 139203. DOI: 10.1007/s11432-019-2893-y

Loria, A. (2015). Observers are unnecessary for output-feedback control of Lagrangian systems. IEEE Transactions on Automatic Control, 61(4), 905-920. DOI: 10.1109/TAC.2015.2446831.

Na, G., Jo, N. H., & Eun, Y. (2019). Performance degradation due to measurement noise in control systems with disturbance observers and saturating actuators. Journal of the Franklin Institute, 356(7), 3922-3947. DOI: 10.1016/j.jfranklin.2019.03.001

Okubanjo, A. A., Oyetola, O. K., Osifeko, M. O., Olaluwoye, O. O., & Alao, P. O. (2017). Modeling of 2-DOF robot arm and control. Futo J Series (FUTOJNLS), 3(2), 80-92.

Pérez Vidal, A. J., Castro-González, Á., Alonso Martín, F., Castillo, J. C., & Salichs, M. Á. (2017). Evolución de la robótica social y nuevas tendencias. Actas de las XXXVIII Jornadas de Automática. http://hdl.handle.net/10651/46926.

Rebouças Filho, P. P., da Silva, S. P. P., Praxedes, V. N., Hemanth, J., & de Albuquerque, V. H. C. (2019). Control of singularity trajectory tracking for robotic manipulator by genetic algorithms. Journal of computational science, 30, 55-64. DOI: 10.1016/j.jocs.2018.11.006.

Sariyildiz, E., & Ohnishi, K. (2014). Stability and robustness of disturbance-observer-based motion control systems. IEEE Transactions on Industrial Electronics, 62(1), 414-422. DOI: 10.1109/TIE.2014.2327009

Shtessel, Y., Edwards, C., Fridman, L., & Levant, A. (2014). Sliding mode control and observation (Vol. 10). New York: Springer New York. DOI: 10.1007/978-0-8176-4893-0.

Stotsky, A., & Kolmanovsky, I. (2001, June). Simple unknown input estimation techniques for automotive applications. In Proceedings of the 2001 American Control Conference. (Cat. No. 01CH37148) (Vol. 5, pp. 3312-3317). IEEE. DOI: 10.1109/ACC.2001.946139.

Urrea, C., Kern, J., & Alvarado, J. (2020). Design and evaluation of a new fuzzy control algorithm applied to a manipulator robot. Applied sciences, 10(21), 7482. DOI: 10.3390/app10217482.

ISSN: 2524-2121
RENIECYT-SECIHTI: 1702902

Pacheco, Jorge, Cortés-Vega, David, Sanchez-Lara, Rafael, Alazki, Hussain. [2025]. PID control for tracking A 5 DOF robotic manipulator subjected to exogenous forces. ECORFAN-Journal Taiwan. 9 [16]1-15: e6916115.
https://doi.org/10.35429/EJT.2025.9.16.6.1.15

Vo, A. T., Truong, T. N., & Kang, H. J. (2021). A novel tracking control algorithm with finite-time disturbance observer for a class of second-order nonlinear systems and its applications. *IEEE Access*, *9*, 31373-31389. DOI: 10.1109/ACCESS.2021.3060381

Yilmaz, B. M., Tatlicioglu, E., Savran, A., & Alci, M. (2021). Self-adjusting fuzzy logic based control of robot manipulators in task space. IEEE Transactions on Industrial Electronics, 69(2), 1620-1629. DOI: 10.1109/TIE.2021.3063970.

Zhang, Z., Zheng, L., Yu, J., Li, Y., & Yu, Z. (2017). Three recurrent neural networks and three numerical methods for solving a repetitive motion planning scheme of redundant robot manipulators. IEEE/ASME Transactions on Mechatronics, 22(3), 1423-1434. DOI: 10.1109/TMECH.2017.2683561.

ISSN: 2524-2121
RENIECYT-SECIHTI: 1702902

Pacheco, Jorge, Cortés-Vega, David, Sanchez-Lara, Rafael, Alazki, Hussain. [2025]. PID control for tracking A 5 DOF robotic manipulator subjected to exogenous forces. ECORFAN-Journal Taiwan. 9 [16]1-15: e6916115.
https://doi.org/10.35429/EJT.2025.9.16.6.1.15